



# Electron Spin Resonance Spectra of Dioxygen and Nitric Oxide

 Igor V Khudyakov<sup>1\*</sup> and Boris F Minaev<sup>2</sup>
<sup>1</sup>Department of Chemistry, Columbia University, USA

<sup>2</sup>Department of Chemistry and Nanomaterials Science, Bohdan Khmelnytsky National University, Ukraine

\*Corresponding author: Igor V Khudyakov, Department of Chemistry, Columbia University, New York, USA

Received: 📅 March 26, 2021

Published: 📅 April 6, 2021

## Abstract

Molecular terms of dioxygen and nitric oxide are presented. Electron spin resonance spectra of diatomic molecules corresponding to these terms are discussed. Gas-phase ESR can be a convenient method of monitoring paramagnetic pollutants in the atmosphere. We ran additional calculations in molecular physics for terms of these molecules and Zeeman transitions.

**Keywords:** ESR; Pollutants; Gas Phase; Terms of Diatomic Molecules; Electronic Structure of Diatomic Molecules; ESR Spectra of Singlet Dioxygen and Nitric Oxide

## Introduction

Pollution of the atmosphere becomes a more and more important problem for humanity every year. Many pollutants have been well-documented in various atmospheric research [1]. It is important to monitor the concentration of pollutants from the standpoint of the safety of a population, air quality, and photochemical smog formation. Some of the pollutants are paramagnetic and demonstrate ESR spectra in the gas phase. In this mini review, we consider the electronic structure and magnetic properties of two pollutants: singlet dioxygen and nitric oxide in the gas and the liquid phase as well as their ESR spectra. It is demonstrated that an X-band ESR is a promising tool for detection and monitoring these two pollutants.

## Electronic Terms of Dioxygen and Nitric Oxide

The molecular term symbol of the ground and some excited state of these diatomic radicals are determined in a short presentation by the total electronic spin angular momentum ( $S$ ), by its projection  $S_z$  on the molecular  $z$ -axis ( $\Sigma$ ) [2], by the orbital angular momentum  $z$ -projection ( $\Lambda$ ), as well as their sum - total electronic momentum projection  $J = S_z + \Lambda$  [2-4]. The quantum numbers for the observed values of projections of these momenta on the internuclear axis of a diatomic molecule are denoted as  $J, \Sigma$  and  $\Lambda$ , respectively and  $J = |\Lambda + \Sigma|$ . According to a common convention [2-6], the states with  $\Lambda = 0, 1, 2$  are denoted by  $\Sigma, \Pi, \Delta$  symbols. (One should distinguish notations of spin projection and the case of  $\Lambda = 0$ ,

which are denoted by the same symbol  $\Sigma$ ). The quantum numbers, which determine the measured absolute value of the total spin and its projection on the  $z$ -axis are fixed in the quantum theory of angular momentum as eigenvalues of the corresponding square  $S^2$  operator and the  $S_z$  operator [5]:

$$S^2\Psi = S(S+1)\hbar^2\Psi; S_z\Psi = \Sigma\hbar\Psi, \quad (1)$$

Where  $\hbar$  is  $\hbar = h / 2\pi$  as usual and  $h$  is the Planck constant.

For the singlet  $^1O_2(^1\Delta_g)$  and triplet  $^3O_2(^3\Sigma_g^-)$  state dioxygen the spin quantum number is equal to  $S=0$  and  $S=1$ , respectively. In the last case, the spin projection quantum number has values  $\Sigma = 0, \pm 1$ . For the zero-spin singlet state the projection is naturally absent ( $\Sigma = 0$ ). In the case of the ground state  $^2NO$  radical  $S = 1/2$ ,  $\Sigma = \pm 1/2$  and two  $\Omega$  values are possible ( $3/2$  and  $1/2$ ). For analysis of ESR and optical spectra of diatomic molecules, one must consider rotational angular momentum  $R$  [2-4]. Because of the axial symmetry of the field in diatomic molecules, only the orbital angular momentum projection of electrons on the  $z$ -axis can be observed as a constant of motion [2]. For the  $\pi^2$  open shell of dioxygen there are two possibilities for the electronic wave functions  $\Psi$  of states with  $\Lambda = 0$ ; function  $\Psi$  can either change sign upon reflection in any plane, which contains internuclear axis  $z(\Sigma^- \text{State})$  or does not change sign  $z(\Sigma^+ \text{State})$ . These symmetry restrictions relate to a general property of all electrons in respect to their permutation [4, 5]. For the triplet state ( $^3\Sigma^-$ ), the spin part of the wave function

is symmetric, but the spatial part is asymmetric, in respect to permutation; this leads to a sign change upon reflection in a molecular plane since  $\pi^+$  transforms to  $\pi^-$  [4]. Terms may include one or two additional notions related to operations of symmetry of a molecule, namely g/u for homonuclear diatomic species, like  $O_2$ , with the inversion symmetry center or +/- in case  $\Lambda = 0$ . We will present the terms including these notations like it is presented in the literature [2-6]. The two additional notations are unimportant in the context of this mini review. The contribution of nuclear momentum **I** and rotational momentum **R** into **J** are mostly omitted here since main isotope  $^{16}O$  has no nuclear spin and for the  $^1O_2(^1\Delta_g)$  molecule we will consider the ESR spectrum for the lowest rotational state  $R=0$ . Detailed information on the terms of diatomic molecules can be found in ref. [2-6].

The terms are presented as  $^{2S+1}\tilde{E}J$ ;  $S$  of one electron is  $1/2$  and  $M_s = \pm 1/2$ . The total spin quantum number  $S$  is used in the superscript

of a term to denote the term multiplicity  $m=2S+1$ . Thus  $^1\Lambda_j$ ,  $^2\Lambda_j$ , and  $^3\Lambda_j$  correspond to a singlet state, doublet state (a radical), and a triplet state of a diatomic molecule, respectively. We deal with two molecules that have the highest occupied  $2\pi^*$  molecular orbital - antibonding  $\pi$ -orbitals. The individual electron on two degenerates  $\pi^*$ - orbitals have a projection of orbital momentum as quantum number  $\lambda_i = \pm 1$ . When we deal with two degenerates  $\delta$ - orbitals, it is necessary to ascribe  $\lambda_1 = \pm 1$  to an electron on one orbital and  $\lambda_2 = 1$  to another. Projection of a total orbital momentum for two electrons in the open  $2\pi^*$  shell  $\Lambda = \lambda_1 + \lambda_2$  is denoted  $\Sigma$ ,  $\Pi$ , and  $\Delta$  for  $\Lambda = 0, 1$ , and  $2$ , respectively. ESR studies of dioxygen and nitrous oxide have been performed by numerous researchers [7-18], but for their practical application in analytical purposes, we need to generalize common physical backgrounds and clarify some details, which have not been considered yet.

We discuss the individual terms of (Table 1) below.

**Table 1:** The terms of  $O_2$  and  $^2NO$  in the ground and the closest in energy excited states as well as their paramagnetic in the gas and the liquid phases.

Molecule	Ground state term	ESR <sup>1</sup> in the following state	Term of the nearest excited state	ESR <sup>1</sup> in the following state
$O_2$	$^3\Sigma_g^-$	Liquid: <b>No</b> <sup>2</sup>	$^1\Delta_g$	Liquid: <b>No</b>
		Gas: <b>Yes</b>		Gas: <b>Yes</b> <sup>3</sup>
$NO$	$^2\Pi_{1/2}$	Liquid: <b>No</b>	$^2\Pi_{3/2}$	Liquid: <b>No</b>
		Gas: <b>No</b>		Gas: <b>Yes</b>

<sup>1</sup>X-band spectrometer.

<sup>2</sup>See the text below.

<sup>3</sup>Electronically-excited state

The terms of heteronuclear diatomic radicals  $^2\Pi_n$  (like the ground state of  $^2NO$  molecule) have index  $\Omega = \Lambda + S_z$ . Typical values of  $\Omega$  are  $1/2, 3/2$ . (We simplify the situation by ignoring molecular rotation in this case, which is acceptable for our goal.) Transitions between different states in ESR spectra are allowed at  $\Delta M_J = \pm 1$ .

## Dioxygen

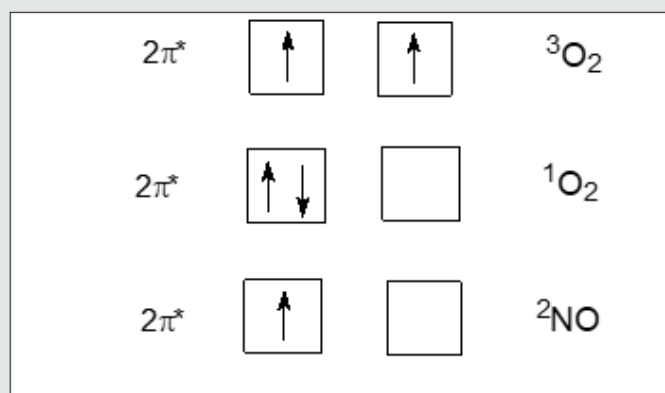
Molecular oxygen (dioxygen) possesses a ground triplet state  $^3O_2(^3\Sigma_g^-)$ . Triplet dioxygen  $^3O_2$  demonstrates a very broad (width of ca. 1 T [7]) weak ESR spectrum in the liquid phase at low temperatures. Orbital angular momentum has a large contribution to the magnetism of molecules and in the case  $^3O_2(^3\Sigma_g^-)_{\Lambda=0}$ . Also, molecular rotations are quenched by the solvent. ESR of  $^3O_2$  is not observed in liquid solutions at room temperature. Molecules in the gas phase undergo free rotation. At the same time, they have quantized energy levels [2]. Rotation of a molecule leads to the appearance of local magnetic fields, and these fields interact with an electronic spin magnetic moment in triplet state  $^3O_2(^3\Sigma_g^-)$  and with orbital magnetism in the excited singlet  $^1O_2(^1\Delta_g)$  dioxygen. The rotation levels make an infinite ladder of spin-energy levels and

rotational levels are in separately interlaced with magnetic levels [2]. That way the ESR spectrum of  $^3O_2$  consists of a huge number of components (lines). An intensive ESR spectrum is observed in the gas phase under low pressure, see (Figure 1).

The nearest in energy to the ground triple  $^3O_2(^3\Sigma_g^-)$  dioxygen is the electronically excited state. it provides another ESR spectrum (see Scheme 1 and Table 1). Singlet dioxygen is 94 kJ/mol above the triplet ground state. There are many ways to generate labile singlet dioxygen [9,10,12-14,17,19]. Singlet molecule does not have spin ( $S=0$ ) but has an electronic orbital angular momentum  $\Lambda = 2$  [9-17]. Together with the rotational angular momentum (**K**), they form a total angular momentum  $\mathbf{J} = \Lambda + \mathbf{K}$ ; it is quantized along the magnetic field axis with quantum number  $M_J$ . The molecule belongs to the classical Hund's case (a) when  $\Lambda$  is quantized along the molecular z-axis [2]. Values and  $J$  in this case are good quantum numbers [3]. Thus, for free rotating  $^1O_2(^1\Delta_g)$  molecule in the gas phase, the total momentum **J** provides ESR spectrum [9,13]. The  $\Lambda$ -doubling in the  $^1O_2(^1\Delta_g)$  molecule is expected to be very small [4,18], in fact neither we nor other authors [19] could resolve the doubling splitting in the singlet oxygen ESR spectrum.

Zeeman energy of  $^3\text{O}_2(^3\Sigma_g^-)$  in an external magnetic field  $H$  can be described by the following equation for magnetic field interaction with molecular magnetic moment [13,23]:

$$E_J = \mu_B g_L H M_J \frac{(\Lambda + 2\Sigma)(\Lambda + \Sigma)}{J(J+1)} = \mu_B H M_J g_J \quad (2)$$



**Scheme 1:** below presents an occupation of the highest molecular orbitals by electrons in these two species.

The spin angular momentum projection is absent ( $\Sigma=0$ ) for the singlet dioxygen and we have a relation:  $g_J = g_L \Lambda^2 / J(J+1)$ . For the lowest rotational level ( $J=\Lambda=2$ ) we have  $g_J = 2g_L/3$  [13]. The electronic magnetic moment along molecular axis  $z$  is equal  $2g_L \mu_B$ , where  $\mu_B = e\hbar/2mc$  is the Bohr magneton and  $g_L$  is the electronic orbital angular momentum  $g$ -factor, which is close to unity [13]; small corrections to  $g$ -factor of the singlet  $^1\text{O}_2(^1\Delta_g)$  state are important for the ESR spectrum and are considered below. Since  $g_L \approx 1.0$  and  $g_J \approx 2/3 \approx 0.667$ , all allowed transitions with  $\Delta M_J = \pm 1$  in the ESR spectrum of  $^1\text{O}_2(^1\Delta_g)$  dioxygen should have the same transition energy about  $\frac{2}{3} \mu_B H$ . Only one transition  $0 \rightarrow 1$  is close to the  $0.667 \mu_B H$  resonance [23], but all others are shifted [9].

In the absence of electron-rotational interaction, all four ESR transitions in the ground state ( $J=\Lambda=2$ ) of the singlet  $^1\Delta_g$  dioxygen would be observed at the same field about  $H \approx 10$  kG with the frequency (9624.92 MHz) of X-band ESR spectrum. Transition's

energies  $h\nu_i$  in the ESR spectrum (Figure 1) are different (at a fixed field  $H$ ) because of perturbations from the upper rotational  $J=3$  levels (Figure 2). They are equal to 0.65597 for  $(-2 \rightarrow -1)$  transition, 0.66264  $(-1 \rightarrow 0)$ , 0.66954  $(0 \rightarrow +1)$  and 0.67667  $(+1 \rightarrow +2)$  in the units  $\mu_B H$  [9,13]. Thus, we have almost symmetrically split quartet ESR lines (Figure 1). At the fixed microwave frequency  $\nu = 9.62492$  GHz the EPR X-band resonance signals are obtained at the magnetic field strength about  $H \approx 10$  kG, respectively [9]. Account of interaction with the first excited rotational level  $K=1$  ( $J=3$ ) provides additional corrections to  $M_J$  sublevels of the ground rotational state  $J=2$  in the second order of perturbation theory; the results are presented in (Figure 2) below [13]. One can see from Table 2 and Figure 2 that the splitting between nearest transitions is equal to  $2a$ , that the splitting between nearest transition is equal to  $2a$ .  $a$  value is presented below (Figure 2) and is energy of the splitting:

$$a = (2\mu)H^2/379B_e, \text{ where } B_e \text{ is a rotational constant.}$$

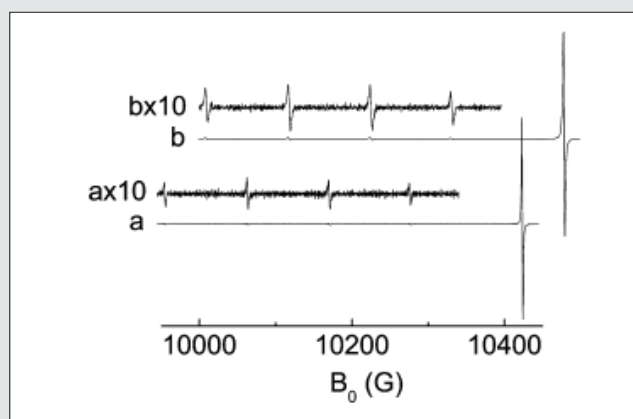


**Figure 1:** The ESR spectra in the sealed cell containing  $^3\text{O}_2$  ( $P_{\text{O}_2} = 0.2$  Torr) and a sensitized- naphthalene vapor obtained in the dark (a) and during irradiation of a sensitizer (b),  $T = 293$  K. The intensity component in the high field (a, b) is part of the ESR of  $^3\text{O}_2(^3\Sigma_g^-)$ . The ESR spectrum of  $^1\text{O}_2(^1\Delta_g)$  consisting of four components (b and bx10) was obtained under photoexcitation of naphthalene in the presence of  $^3\text{O}_2$ . Adapted from ref [9].

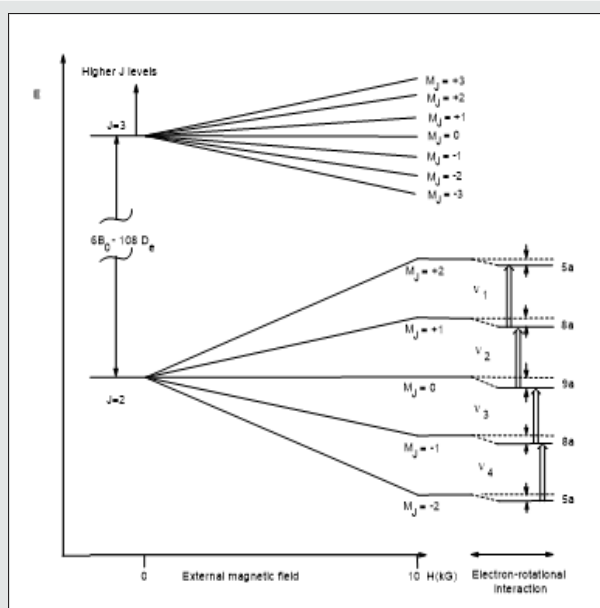


Figure 2: Splitting of the ground and first excited rotational levels of the singlet oxygen  ${}^1\text{O}_2({}^1\Delta_g)$  state in magnetic field  $H$ . Generalized from refs [13,23].

Table 2: Second-order corrections for  $J=2$  of  ${}^1\text{O}_2({}^1\Delta_g)$  spectrum of the X band ESR signals Observed [9].

ESR Transition	Field (G)	$h\nu_i / \mu_B H^1$	$h\nu_i / \mu_B H^2$	Second-order correction <sup>2</sup>
(-2 → -1)	10 486.00	0.655	0.65597	$\nu_0 + (5 - 8)a$
(-1 → 0)	10 375.68	0.662	0.66264	$\nu_0 + (8 - 9)a$
(0 → +1)	10 264.67	0.669	0.66954	$\nu_0 + (9 - 8)a$
(+1 → +2)	10 151.75	0.677	0.67667	$\nu_0 + (8 - 5)a$

<sup>2</sup>Calculated by second-order correction [12,23]

which depends on the ratio of magnetic field  $H^2$  and rotational constant  $B_e$ . This prediction agrees well with the observed quartet splitting in ESR spectra of singlet dioxygen in the gas phase [9,13,23].

There is no ESR spectrum of  ${}^1\text{O}_2({}^1\Delta_g)$  in the liquid phase since the local electric fields of solvent molecules quench the orbital angular momentum [2]. At any oxygen collision with a solvent molecule, the local electric fields remove the degeneracy of the state; it splits into two close-lying sublevels which position depends on the geometry of any new collision and orbital angular momentum  $\Lambda$  is not anymore, a good quantum number. (Non-zero orbital angular momentum can exist only in degenerate states) [21]. Thus, the simple Zeeman energy picture, equation (1), is completely distorted and rotational coherence is quenched. High accuracy of ESR measurement in the gas phase provides a good agreement between perturbation theory and the observed quartet splitting in the ground rotational level  $J=2$  of singlet oxygen [13,23]. But this accuracy leads to additional problems with exact values of  $g_L$ -factor.

Rotational  $g_L$ -factor contains small contributions from relativistic mass-velocity dependence [23] and non-diagonal orbital momenta terms responsible for mixing of different states induced by the shift operator  $L_+$  and  $L_-$ . Similar contributions in combination with spin-orbit coupling (SOC) perturbation are responsible for anisotropy of electronic spin  $g$ -factor; they are rather important for the ground triplet state of dioxygen  $\Lambda$  and provide ESR signal deviation from the free-electron value ( $g_e = 2.0023$ ). This deviation is big for perpendicular component of  $g$ -tensor (as much as  $g^\perp = 2.0052$  [3, 22]), while  $g^\parallel$  is close to  $g_e$  value [20,24]. These parameters were first obtained from the ESR spectrum of solid dioxygen [3] and these parameters are supported by *ab initio* self-consistent field (SCF) calculations [22,24]. Electronic spin  $g$ -factor relates to the spin-rotational coupling constant ( $\gamma$ ) approximation is well developed for the ground and excited triplet states  ${}^3\Sigma^-$  of dioxygen [24]. But for the singlet  ${}^1\text{O}_2({}^1\Delta_g)$  molecule the rotational  $g$ -factor theory contains some discrepancies which should be shortly discussed [13,23], which will be briefly discussed in the next section.

## A Short Introduction to the Theory of Rotational g-Factor for the Singlet $^1\text{O}_2(^1\Delta_g)$ Molecule

Rotational  $g_L$ -factor includes nuclear part  $g_r^N$  and the orbital part  $g_r^e$  [26]. The nuclear rotational g-factor is simply determined by atomic mass ( $M_A$ ) and charge ( $Z_A$ ); it corresponds to the moment for bare nuclei of two atoms A and B [4]. It does not contribute to the energy of the lowest rotational level  $K=0$  of the  $^1\text{O}_2(^1\Delta_g)$  molecule.

$$g_r^N = m_p \frac{Z_A M_B^2 + Z_B M_A^2}{(M_A + M_B) M_A M_B} = 2.723 \times 10^{-4} \quad (3)$$

The orbital part in the first order of perturbation theory is equal [26]:

$$g_r^e = \frac{2m_p}{m_e \mu R^2} \sum_{n \neq 0} \frac{|\langle \Psi_0 | \sum_i l_{i,\perp} | \Psi_n \rangle|^2}{E_0 - E_n}, \quad (4)$$

where  $m_p, m_e, \mu$  are a mass of proton, electron and reduced mass of dioxygen,  $R$  is the inter-nuclear distance,  $l_{i,\perp}$  is the perpendicular component of the orbital angular momentum operator for the  $i$ -th electron,  $\Psi_n, E_n$  are eigenfunction and energy of the  $n$ -th singlet state of  $\text{O}_2$  [24-26]. The main contributions to the sum (3) provide  $^1\Pi_g, ^1\Phi_g$  states [24]. The lowest state produces the largest contribution ( $-3.143 \times 10^{-4}$ ) at the equilibrium  $R_e$  distance [26]. Complete active space (CAS) linear response calculations [24] predict a value of  $-3.896 \times 10^{-4}$ , which is in a good agreement with the experimental estimation of  $(-3.957 \pm 0.025 \times 10^{-4})$  obtained in reference [23]. Electronic rotational  $g_r^e$ -factor represents magnetic moment produced by rotation of "electrons following the nuclei" during molecular rotation [13]. Together with angular momenta  $\Lambda$  and  $K$ , it forms the total angular momentum  $J$ ; the late being quantized along the axis of a magnetic field with quantum number Miller [23] has compared this electronic rotational  $g_r^e$ -factor for the  $^1\text{O}_2(^1\Delta_g)$  state with  $g_r^e$ -value for the ground  $^3\text{O}_2(^3\Sigma_g^-)$  states [ $-3.98 \pm 0.12 \times 10^{-4}$ ], also extracted from experiment (3), and noted their similarity within experimental errors.

Arrington et al. [13] have obtained S-band ESR spectra at 3 GHz for  $J=2$  and  $J=3$  levels (only two of six transitions for  $J=3$  spectrum has been detected because of high field resonances). The  $g_J = 4g_L / J(J+1)$  values obtained from the S-band spectra are consistent within the  $H$  field measurement error; for the  $J=2$  spectrum, these g-factors are much more accurate [19] than those obtained from the X-band ESR data [8]. The averaged  $g_J$  values for  $J=2$  are equal to 0.66663 and for  $J=3$  it is 0.33340 in the S-bands ESR components [13]. Then the authors [13] have solved a system of two equations for two  $J$  values  $\frac{2}{3}g_L - \frac{1}{3}g_r = g_J$  for  $J=2$  and  $\frac{1}{3}g_L - \frac{2}{3}g_r = g_J$  for  $J=3$  and found finally  $g_r = -1.70 \times 10^{-4}$  ( $g_L = 0.99986$ ). The last value for  $g_L$  of Arrington et al. [13] is in good agreement with more accurate full EPR spectrum analysis of Miller [23], but the rotational  $g_r$ -factor resolved by Miller is different  $g_r = (-1.234 \pm 0.025) \times 10^{-4}$ , which is outside an experimental error [13,23]. Thus, the orbital magnetic

moment of the  $^1\text{O}_2(^1\Delta_g)$  molecule is slightly different from a simple  $2\mu_B$  value and this difference is crucial for the splitting between the quartet ESR lines, which appear through the second-order corrections [23]. We will remind that  $g_r = g_r^e + g_r^N + g_r^e + 2.723 \times 10^{-4}$ , which is outside the experimental error; thus, the rotational  $g_r$ -factor represents a difference between two comparable values. Electronic contribution ( $g_r^e$ -factor) being almost equal to  $-3.96 \times 10^{-4}$  for the  $^1\text{O}_2(^1\Delta_g)$  state and simultaneously close to  $g_r^e$ -value for the ground state of dioxygen  $^3\text{O}_2(^3\Sigma_g^-)$  leads to some doubts of researchers since equation (3) provides different origins for both states [13,23]. Indeed, only  $^3\Pi_g$  states of  $^1\text{O}_2$  can contribute to the  $g_r^e$ -value for the ground triplet dioxygen [22,26].

The excited  $^1\text{O}_2(^1\Delta_g)$  is usually produced in the presence of great excess of the triplet ground state oxygen [9,27]. Thus, both ESR signals appear simultaneously in the same magnetic field ranges and the triplet ground state oxygen lines are used as an internal standard for the singlet excited  $^1\text{O}_2(^1\Delta_g)$  concentrations measurements [9,13]. But the nature of the ESR signal for both states of dioxygen  $^3\Sigma_g^-$ ;  $\Lambda = 0$ ; and  $^1\Delta_g$ ,  $\Lambda = 2$ , is rather different. The triplet state ESR transitions frequency is determined by spin g-factor ( $g^+ = 2.0052$ ) and by its anisotropy with  $g^{\parallel} = g_e$  parameter induced by spin-orbit coupling SOC mixing, while the dioxygen exhibits nearly symmetric quartet splitting due to the electron-rotational interaction when O-O bond axes rotates around two perpendicular directions. In the late case a value of rotational  $B_e$  constant determines the spitting of the quartet lines. Understanding of this difference is essential for the choice of the field strength  $H$  and microwave ESR frequency range for detection of both the ground  $^3\text{O}_2(^3\Sigma_g^-)$ , and the excited  $^1\text{O}_2(^1\Delta_g)$  dioxygen.

Intensity analysis of the  $^1\text{O}_2$  singlet-triplet transitions in the visible ( $\lambda$  760 nm) and near IR ( $\lambda$  1.27  $\mu\text{m}$ ) regions indicates that these bands have a magnetic-dipole origin and are induced by spin-orbit coupling (SOC) [21, 22]. In optical spectroscopy, the ground is denoted by the letter X and excited states of other multiplicity are enumerated by small Latin letters  $a, b$ , etc. [4]. The weak intensity of the  $^3\text{O}_2(X^3\Sigma_g^-) \rightarrow ^1\text{O}_2(a^1\Delta_g)$  band is determined by the same SOC-induced mixing with the  $^3\Pi_g$  states which are responsible for rotational  $g_r^e$ -values in the ground triplet and the singlet excited  $\text{O}_2$  states with similar contributions of the orbital angular momentum, equation (3) [33-35]. At the same time, the spin g-factor of the state also depends on the similar orbital angular momentum contributions [22,33]. A good agreement of all these calculations with experimental ESR and optical data support the reliability of the similar  $g_r^e$ -values for both  $^3\text{O}_2(X^3\Sigma_g^-)$  and  $^1\text{O}_2(a^1\Delta_g)$  states.

## Nitric Oxide

Let us consider a free radical  $^2\text{NO}(^2\Pi_{1/2})$ , see Scheme 1 and Table 1. It has  $S = 1/2, S_z = \pm 1/2, \Lambda = 1$ . The total angular momentum about the molecular axis (neglecting rotation) is defined as  $J = |\Lambda + S_z|$ . The lowest state of  $^2\text{NO}$  radical has  $J = 1 - 1/2 = 1/2$ . Since the open-shell is occupied less than one-half (double degenerate two  $\text{MO}_s$  has only one electron) we get the regular SOC-induced coupling

splitting [39]. A formula for the spin g-factor of a diatomic radical has a factor  $(\Lambda - 2S)$  which is 0 for the current state [13]. That means state has  $g=0$  and is diamagnetic in both gas and liquid states due to a cancellation of orbital and spin angular momenta.

The next excited state of  ${}^2\text{NO}$  is  ${}^2\Pi_{3/2}$ , where  $s = 1/2, \Lambda = 1$ . This state has  $J = 1 + 1/2 = 3/2$ .  $J=3/2$  splits into four sublevels  $M_J = -3/2, -1/2, +1/2, +3/2$ . Thus, one expects three ESR transitions with the following changes in  $M_J$ :  $-3/2 \rightarrow -1/2$ ;  $-1/2 \rightarrow +1/2$ ;  $+1/2 \rightarrow +3/2$ . The first spectra of  ${}^2\text{NO}$  ( ${}^2\Pi_{3/2}$ ) demonstrated namely 3 components [2,7,10]. Non-magnetic  ${}^2\Pi_{1/2}$ , and paramagnetic states of  ${}^2\text{NO}$  are very close in their energies. The excited state  ${}^2\Pi_{3/2}$  is only 1.43 kJ/mol higher in energy than the ground  ${}^2\Pi_{1/2}$  state [14]. Let us consider the factors, which determine this energy splitting. The open-shell wave function of the doublet  ${}^2\Pi_J$  state can be presented in the following forms: for the case of less-than-half occupied open  $\pi$ -shell we use equation (4), and equation (5) - for the case of more-than-half occupied  $\pi$ -shell [39].

$${}^2\Pi_J = \frac{1}{\sqrt{2}}(\pi_x \pm i\pi_y) \quad {}^2\Pi_J = \frac{1}{\sqrt{2}}(\pi_x \mp i\pi_y) \quad (5)$$

$${}^2\Pi_J = \frac{1}{\sqrt{2}}(|\pi_y \bar{\pi}_y \bar{\pi}_x | \mp i | \pi_x \bar{\pi}_x \bar{\pi}_y |) \quad (6)$$

The upper sign in these equations corresponds to  $J=3/2$  and the lower sign corresponds to  $J=1/2$ . The imaginary form of wavefunction is necessary to satisfy the requirement  $L_z \Psi = \Lambda \hbar \Psi$ . We use here a common notation for the Slater determinant of many-electron wave function [5]. Spin-orbit coupling (SOC) operator can be used in a simple effective single-electron form [29,30]

$$H_{SOC} = \sum_i \sum_A \zeta_{n,i}^A \vec{l}_i \cdot \vec{s}_i = \sum_i \vec{B}_i \cdot \vec{s}_i \quad (6)$$

where  $\zeta_{n,i}^A$  is the SOC constant for the valence shell of atom  $A$ ,  $\vec{l}_i$  and  $\vec{s}_i$  are orbital and spin angular momentum operators, respectively for the  $i$ -th electron. The SOC constants obtained from atomic spectra are equal  $\zeta_{2p}^N = 73 \text{ cm}^{-1}$  and  $\zeta_{2p}^O = 153 \text{ cm}^{-1}$  for nitrogen and oxygen, respectively [29]. Since  $J = |\Lambda + S_z|$ , there are two possible presentations for each  $J$ . Expectation energy of the

SOC operator is equal

$$\varepsilon_J = \langle {}^2\Pi_J | H_{SOC} | {}^2\Pi_J \rangle = \pm \frac{1}{4} [\langle \pi_x | B_z | \pi_y \rangle - \langle \pi_y | B_z | \pi_x \rangle] \quad (7)$$

Let us take  $2\pi^*$ - molecular orbital of  ${}^2\text{NO}$  radical from the SCF calculation with the zero differential overlap approach within PM-3 method [32]:  $2\delta_{x(y)} = 0.811\Psi_{P_{x(y)}}^N - 0.585\Psi_{P_{x(y)}}^O$ . This form of  $2\pi$ -MO is in good agreement with the hyperfine coupling parameters fitting to ESR spectrum of gaseous  ${}^2\text{NO}$  molecule [31]. Using these MO LCAO ( $C_{P_{x(y)}}^A$ ) coefficients we obtain the following splitting:

$$\varepsilon_{3/2} - \varepsilon_{1/2} = \sum_A (C_{P_{x(y)}}^A)^2 \zeta_{2p}^A = 100.4 \text{ cm}^{-1} = 1.2 \text{ kJ/mol} \quad (8)$$

which is in a reasonable agreement with the experiment [20]. Even such a simple semi-empirical approach provides a quantitative explanation of the fine structure SOC splitting in  ${}^2\text{NO}$  radical.  ${}^2\Pi_{3/2}$  is easily accessible at room and lower temperatures; the thermal energy at room temperature is 2.5 kJ/mol. Thus, one can observe the X-band ESR spectrum of the excited  ${}^2\Pi_{3/2}$  state, which is presented in Figure 3 below. One can see that each of the three major components splits into three components due to hyperfine coupling (HFC) with  ${}^{14}\text{N}$  nucleus. A highly resolved spectrum of  ${}^2\text{NO}({}^2\Pi_{1/2})$  has 27 components due to additional interactions [10]. We have calculated the HFC tensor for  ${}^{14}\text{N}$  isotope of  ${}^2\text{NO}$  radical by density functional theory with B3LYP/6-311++G(dp) approach [32]; the isotropic HFC constant  $a = 11.386 \text{ MHz}$ , anisotropic HFC tensor component along the z-axis is equal 74.673 MHz, the oxygen atom bears an electric charge +0.091 e and spin density 0.286, whereas the nitrogen has -0.091 e and 0.714, respectively. Other spectroscopic parameters are in a good agreement with experiment [20]:  $r_e = 1.148 \text{ \AA}$ ,  $\nu_e = 1980 \text{ cm}^{-1}$ ,  $B_e = 51.364 \text{ GHz}$ , averaged polarizability  $\alpha_{av} = 9.4 \text{ a}_0^3$ , dipole moment is equal -0.13 debye. The relatively small polarity and polarizability of  ${}^2\text{NO}$  radical explain its rather weak intermolecular interaction in gas phase; thus, its ESR spectrum at moderate pressure does not depend on properties of foreign gases. The calculated HFC tensor of  ${}^2\text{NO}$  radical with natural isotope abundance does not contradict to experimental ESR spectrum (Figure 3) [10].

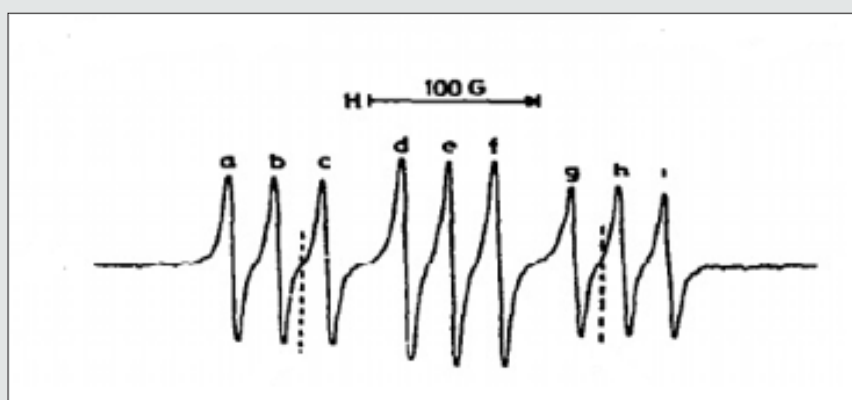


Figure 3: ESR spectrum of  ${}^2\text{NO}$  ( ${}^2\Pi_{3/2}$ ) at room temperature and pressure  $P_{\text{NO}} = 0.5 \text{ Torr}$ . Vertical dashed lines mark the central part of the spectrum. Adapted from ref [10].

The first EPR spectrum of nitric oxide,  ${}^2\text{NO}({}^2\Pi_{1/2})$  was tentatively interpreted as being due to traditional magnetic-dipole transitions (MDT), since the MDT nature is typical for EPR signals [10]. But latter the electric-dipole transitions (EDT) were shown to be more intense and prominent in this EPR spectrum. As many other  ${}^2\Pi$  states the  ${}^2\text{NO}({}^2\Pi_{3/2})$  state, demonstrates a clear  $\Lambda$ -doubling effect t as many  ${}^2\Pi$  states do [14]. The EDT lines occur between opposite members of a  $\tilde{E}$ -doublet ( $- \leftrightarrow +$ ), while much weaker MDT transitions connect the same-doublet members ( $- \leftrightarrow -$ ) or ( $+ \leftrightarrow +$ ) [4]. All these features are determined by relatively strong SOC (equation 8) in quasi degenerate  $2\pi_x$ - and  $2\pi_y$ - molecular orbitals of nitric oxide.

It is interesting to note that in homonuclear dioxygen molecule all EDTs are strongly forbidden by the central point (inversion) symmetry and only weak MDT are observed in the low-pressure gas phase in the triplet-singlet  $b-X$  and  $a-X$  transitions in the visible and near IR regions [21]. But the release of symmetry restriction in solvents permits the  ${}^3\text{O}_2({}^3\Sigma_g^-) \rightarrow {}^1\text{O}_2({}^1\Delta_g)$  band at 1.2  $\mu\text{m}$  to acquires EDT character and become much more intense because of the strong SOC inside the dioxygen  $\sigma_x(\pi_x)$  open shell [28]. Thus, many peculiarities of the optical and EPR spectra of two diatomic species,  ${}^2\text{NO}$  and  ${}^1\text{O}_2$ , being very important for the atmospheric problems, strongly depend on spin-orbit coupling in  $2\pi^*$ - orbitals (Scheme 1) which energy does not exceed 1-2 kJ/mol [21,30]. Spin and rotational energies depend upon each other. Collisions of  ${}^2\text{NO}$  with solvent molecules lead to a spin relaxation or an infinite boarding of components. Note, that gas-phase ESR spectra are observed at low pressure. An increase in pressure leads to the broadening of components.

## ESR of Trapped ${}^2\text{NO}$

${}^2\text{NO}$  is used as a probe of surfaces, different cages, nano-objects, and biological species. Adsorption of  ${}^2\text{NO}$  on surface vacancies, inside

zeolites [11, 15], or the  $\text{C}_{60}$  cavity [16], complexation with biological molecules [18] leads to quenching of the orbital momentum; thus, the lowest  $2\Pi_{1/2}$  state of  ${}^2\text{NO}$  becomes paramagnetic and demonstrates ESR. In the adsorbed  ${}^2\text{NO}$  species, the  $2\pi_x$ - and  $2\pi_y$ - molecular orbitals (MO) are split by interaction with the surface and the energy splitting between the perturbed  $2\pi_x$  and  $2\pi_y$  MO is a measure of the spin g-factor anisotropy [11].  ${}^2\text{NO}$  species is not any more an object of diatomic spectroscopy with proper quantization of orbital and rotational angular momenta. Instead, the polyatomic cluster is an object of the ground and excited states studies. The principal values of g tensor are used now to determine the MO splitting to characterize the electric field strength at the  ${}^2\text{NO}$  adsorption site. An example is presented in (Figure 4): The sharp downwards components (Figure 4) arise due to hyperfine coupling on  ${}^{14}\text{N}$  nucleus of a bound  ${}^2\text{NO}$  and the g-factor just shows the position of the ESR signal. In order to get interpretation of the ESR spectrum in (Figure 4) we have simulated the  ${}^2\text{NO}$  complex with hemoglobin model by quantum chemical DFT calculation (Figure 5) in the framework of B3LYP/6-31 G approach [32]. The Fe-N coordination bond length is optimized to be 0.1866 nm with the angle Fe-N-O = 121.4°, the distance Fe-Cl = 0.2186 nm just simulates the Fe ion coordination with the protein residue. The calculated g-factor has components 2.0137, 2.0082, and 1.9843, which are in a qualitative agreement with the ESR spectrum in Figure 4. A large portion of nonpaired spin is concentrated on Fe ion. The calculated isotropic HFC constant on the  ${}^{14}\text{N}$  nucleus is equal  $a=15.78$  MHz; anisotropic HFC tensor components are calculated at -30.2, -7.3, and 37.5 MHz. Thus, the Fermi-coupling  $a$  constant is slightly increased by 4.4 MHz in comparison with free  ${}^2\text{NO}$  radical, but the components of the HFC tensor are approximately half diminished upon  ${}^2\text{NO}$  coordination to the iron center of hemoglobin. The Fe(II) ion provides a rather strong influence on the hyperfine structure of the ESR spectrum of nitric oxide.

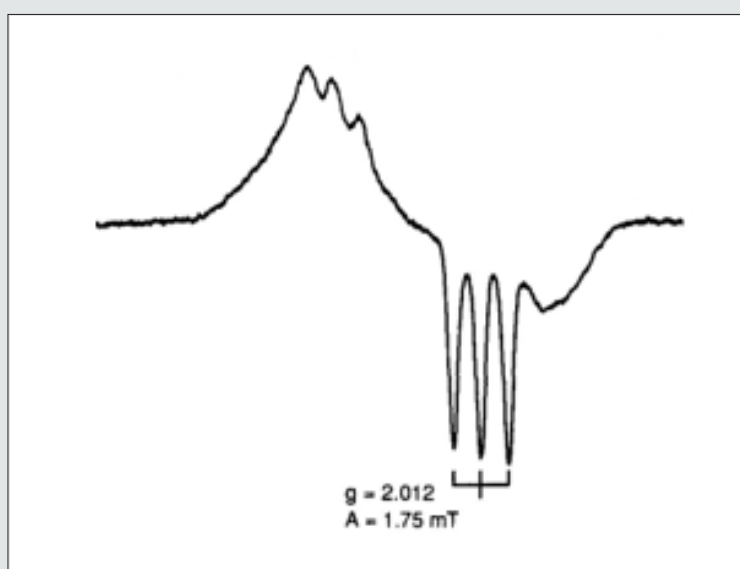


**Figure 4:** ESR spectrum of an adduct of  ${}^2\text{NO}$  and hemoglobin at 90 K. Adapted from references [18]; see for details ref. [18]

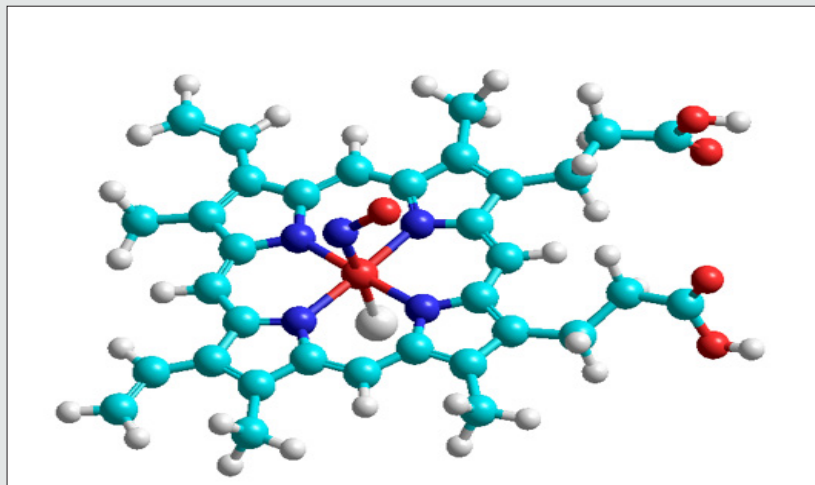


**Figure 5:** The model of the  $^2\text{NO}$  adduct with hemoglobin (coordinated with  $\text{Cl}^-$  anions as a model of protein residue) Red color for O and Fe atoms, dark blue N, blue C, and grey for H atoms. Adapted from reference [34]. This is also a calculation made especially for this paper.

These results are comparable with our previous theoretical DFT studies of  $^2\text{NO}$  and  $\text{O}_2$  interactions with hemoglobin [33,34]. Hyperfine coupling on  $^{14}\text{N}$  nucleus is in agreement with the theory of the nitric oxide ESR spectrum made as early as in 1950 [35].

## Conclusions and Perspectives

A newcomer may be much surprised that a singlet molecule  $^1\text{O}_2$  demonstrates an ESR spectrum in the gas phase. Due to the lack of spin in the molecule, it is better to use the term Electron Paramagnetic Resonance in this case, where paramagnetism is due to the orbital momentum. The radical  $^2\text{NO}$  does not demonstrate the ESR spectrum in liquid solutions. ESR of these and other states can be understood considering the terms of these diatomic molecules.

$^2\text{NO}$  is an atmospheric pollutant.  $^2\text{NO}$  reacts with dioxygen and produces  $^2\text{NO}_2$ , which is a pollutant as well. In the literature on environmental problems, both pollutants are often called  $\text{NO}_x$ .

Air pollutant singlet dioxygen has a relatively short lifetime from milliseconds to less than 10 s [14]. Specific life time depends upon pressure and of the presence of quenchers of  $^1\text{O}_2$ . In the air atmosphere ( $P_{\text{tot}} = 1 \text{ atm}$ )  $^1\text{O}_2$  has a life-time of 2.8 s measured with a quencher [19]. During this time  $^1\text{O}_2$  diffuses approximately 1 cm [19].

The gas pollutants exist in the most cases in the presence of dioxygen. One or another strong line of ESR of  $^3\text{O}_2(^3\Sigma_g^-)$  (Figure 1) can serve as a convenient internal standard for monitoring  $^1\text{O}_2(^1\Delta_g)$  or other gas pollutants.

## Conflict of Interest Statement

There is no conflict of interest.

## References

1. Arnhold, J (2020) Cell and Tissue Destruction. Mechanisms, Protection, Disorders, Academic: London 315-326.
2. Weil JA, Bolton JR, Wertz JE (1994) Electron Paramagnetic Resonance. Elementary Theory and Practical Applications, Wiley: New York 33(1): p. 80.
3. Tinkham M, Strandberg MWP (1955) Theory of the Fine Structure of the Molecular Oxygen Ground State. Phys. physical review journals archive 97(4): 937.
4. Herzberg G (1950) Molecular Spectra and Molecular Structure. I: Spectra of Diatomic Molecules. 1950 Van Nostrand: New York.
5. Murrell JN, Kettle SFA, Tedder JM (1965) Valence Theory, Wiley: London.
6. Khudyakov IV, Serebrennikov, Yu A, Turro NJ (1993) Spin-orbit coupling in free-radical reactions: on the way to heavy elements. Chem. Rev., 93(1): 537-570.
7. Kon H (1973) J Amer Chem Soc 95: 1045.
8. Carrington A (1974) Microwave Spectroscopy of Free Radicals, Academic: London.
9. Ruzzi M, Sartori E, Moscatelli A, Khudyakov IV, Turro NJ (2013) Time-Resolved EPR Study of Singlet Oxygen in the Gas Phase. J. Phys. Chem. A, 117(25): 5232.
10. Jinguiji M, Ohokubo Y, Tanaka I (1978) Chem Phys Lett 54(1): 1-196.
11. Pöpll A, Rudolf T, Manikandan P, Goldfarb D (2000) J American Chem. Soc. 122: 10194.
12. Falick AM, Mahan BH, Myers RJ (1965) Paramagnetic Resonance Spectrum of the  $1\Delta_g$  Oxygen Molecule. J Phys. Chem. 42: 1837.
13. Arrington CA, Falick AM, Myers RJ (1971) J Phys Chem 55: 909.
14. Hasegawa K, Yamada K, Sasase R, Miyazaki R, Kikuchi A, et al. (2008) Chem. Phys. Lett. 457: 312.
15. Lunsford JH (1968) Surface interactions of zinc oxide and zinc sulfide with nitric oxide. Journal of Physics Chemistry 72(6): 2141-2144.
16. Dinse KP, Kato T, Hasegawa S, Hashikawa Y, Murata Y (2020) Magn. Reson. 1: 197.
17. Scalabrin A, Saykally RJ, Evenson KM, Radford HE, Mizushima M, et al. (1981) J Mol.Spectrosc. 89: 344.
18. Westenberer U, Thanner S, Ruf HH, Gersonde K, Sutter G, et al. (1990) Formation of Free Radicals and Nitric Oxide Derivative of Hemoglobin in Rats During Shock Syndrome. Free Rad. Res. Comms, 11(1-3): 167-178.



19. Wang KK, Song S, Jung SJ, Hwang JW, Kim MG, et al. (2020) A two-dimensional h-BN/C2N heterostructure as a promising metal-free photocatalyst for overall water-splitting. *Physical Chemistry Chemical Physics* 22: 24446-24454.
20. Huber KP, Herzberg G (1979) *Molecular Spectra and Molecular Structure. IV. Constants of Diatomic Molecules*. Van Nostrand: New York.
21. Minaev BF (2007) Electronic mechanisms of molecular oxygen activation. *Russ Chem Rev* 76(11): 989-1011.
22. Vahtras, O, Minaev B, Ågren H (1997) *Chem Phys Lett* 281: 186.
23. Miller TA (1971) *J. Phys. Chem* 54: 330.
24. Engström M, Minaev B, Vahtras O, Ågren H (1998) *Chem Phys* 237: 149.
25. Sauer SPA, Hanna Kjær, Jacob Kongsted (2010) Benchmarking NMR indirect nuclear spin-spin coupling constants: SOPPA, SOPPA(CC2), and SOPPA(CCSD) versus CCSD. *J Chem Phys* 133(14): 171101.
26. Minaev BF (1978) Effect of spin-orbit coupling on the intensity of magnetic dipole transitions in molecular oxygen. *Soviet Physics Journal* 21: 1205-1209.
27. Bregnhøj M, Westberg M, Minaev BF, Ogilby PR (2017) Singlet Oxygen Photophysics in Liquid Solvents: Converging on a Unified Picture *Acc Chem Res* 50(8): 1920-1927.
28. Minaev BF (1985) *Optics Spectrosc* 58: 761.
29. Minaev BF (1979) Spin alignment of the triplet state and new methods of the phosphorescence study. *Physics of Molecules Kiev* 7: 34.
30. Minaev BF, Zahradnik R (1981) Calculations of quartet state spectra for diatomic species by INDO CI method including spin-orbit coupling perturbation. *Collection of Czechoslovak Chemical Communication* 46(1): 179-193.
31. Dousmanis, GC (1955) Magnetic Hyperfine Effects and Electronic Structure of NO. *physical review journals archive* 97(4): 967.
32. Frish, M.J. et al. (2009) Gaussian 09, Revision C.02. 2009, Wallingford, CT; Gaussian.
33. Zakharov II, Minaev BF (2011) DFT calculations of the intermediate and transition state in the oxidation of NO by oxygen in the gas phase. *Theoretical and Experimental Chemistry* 47: p. 93.
34. Minaev BF, Minaeva VA (2008) *Ukrain Bioorg Acta*2, 56.
35. Beringzr R, Castle JG (1950) *Phys Rev* 78: 581.

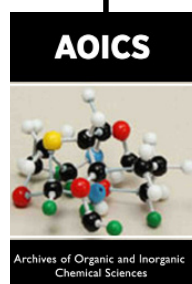


This work is licensed under Creative Commons Attribution 4.0 License

To Submit Your Article Click Here:

[Submit Article](#)

DOI: [10.32474/AOICS.2021.05.000204](https://doi.org/10.32474/AOICS.2021.05.000204)



#### Archives of Organic and Inorganic Chemical Sciences

##### Assets of Publishing with us

- Global archiving of articles
- Immediate, unrestricted online access
- Rigorous Peer Review Process
- Authors Retain Copyrights
- Unique DOI for all articles